



Antibacterial properties of functionalized cellulose extracted from deproteinized soybean hulls

Maria Laura Tummino · Enzo Laurenti · Pierangiola Bracco ·
Claudio Cecone · Valeria La Parola · Claudia Vineis · Maria Luisa Testa

Received: 12 September 2022 / Accepted: 18 June 2023
© The Author(s) 2023

Abstract Soybean hulls (SBHs) are one of the main by-products of soybean crushing, usually destined for animal feeding or to become a putrescible waste. In this work, we upgraded the SBHs to materials with antimicrobial properties. After the extraction of soybean peroxidase from SBHs, an enzyme applicable in different technological sectors and naturally present in soybean hulls, the exhausted biomass was subjected to an acid–base treatment to isolate cellulose. The obtained material was, in turn, functionalized with 3-aminopropyl triethoxysilane (APTES) to achieve new hybrids with antimicrobial properties.

Maria Laura Tummino and Maria Luisa Testa have contributed equally to this work.

Supplementary Information The online version contains supplementary material available at <https://doi.org/10.1007/s10570-023-05339-w>.

M. L. Tummino (✉) · C. Vineis
Institute of Intelligent Industrial Technologies and Systems for Advanced Manufacturing, Italian National Research Council (CNR-STIIMA), Corso G. Pella 16, 13900 Biella, Italy
e-mail: marialaura.tummino@stiima.cnr.it

E. Laurenti · P. Bracco · C. Cecone
Department of Chemistry, University of Torino, Via P. Giuria 7, 10125 Torino, Italy

V. La Parola · M. L. Testa
Institute for the Study of Nanostructured Materials, Italian National Research Council (CNR-ISMN), Via U. La Malfa 153, 90146 Palermo, Italy

The synthetic procedure was optimized by varying the solvent type (ethanol or toluene) and APTES amount. Overall, the amino-functionalization process was effective and the activity was outstanding against both gram-positive and gram-negative bacteria, reaching complete disinfection practically in all cases. The samples were studied by means of several characterization techniques, demonstrating that the solvent and cellulose types had a significant influence on the physical–chemical features, together with the eco-sustainability of the process. In particular, the use of greener ethanol and waste cellulose (with respect to a commercial one) resulted in a higher APTES immobilization efficiency and superior thermal stability of the final materials. Interestingly, the presence of various unremoved compounds from the lignocellulosic SBH matrix, although in small quantities, emerged as a crucial factor, also in terms of antibacterial activity, hypothesizing a role of residual phytochemicals.

Keywords Soybean hulls · Waste cellulose · Amino-functionalization · Antibacterial activity · Sustainability

Introduction

One of the great interests of contemporary research is the production of materials with peculiar characteristics for ad hoc applications in medicine, engineering, energy, and environment. This goal is often reached

by combining compounds of different nature and features, creating new functionalized materials and/or composites. The approach to the preparation of such materials is changing, preferring sustainable synthetic strategies together with natural, renewable, and non-toxic precursors (Bano et al. 2020; Liyanage et al. 2021).

In this direction, cellulose-based materials play an important role in the technological scenario. Cellulose is the most abundant biopolymer in nature and consists of a linear chain of D-glucose units linked by β -1,4-glycosidic bonds (French 2017). Cellulose and its derivatives are the main components of many materials present in our daily life, such as textile fibers (cotton, viscose, flax, jute, etc.), cotton wool, paper, and cellophane (Kumar Gupta et al. 2019). Advanced applications already take advantage of nanocellulose (which comprises micro- and nano-structured cellulose according to the definition of (Trache et al. 2020)) in pharmaceutical and cosmetic formulations, food technology industry, biomedical sector, electronic devices, construction field, and decontamination systems (Shokri and Adibki 2013; Trache et al. 2016, 2020; Kumar Gupta et al. 2019; Reshmy et al. 2020; Testa and Tummino 2021; Nemeş et al. 2022). Cellulose has received considerable attention because it is obtained from renewable and widely available resources; it is non-toxic, biodegradable, low-cost and has favorable physicochemical characteristics that make this compound very versatile (Kwiczak-Yiğitbaşı et al. 2020). The cellulose structure is primarily affected by hydrogen bonds and van der Waals forces. Hydrogen bonding within neighboring cellulose chains may determine the straightness of the chain and impart improved mechanical properties and thermal stability (Poletto et al. 2013). The latter is regulated by crystallinity index, crystallite size and degree of polymerization (Poletto et al. 2013). Cellulose chemical reactivity is mainly determined by the presence of hydroxyl groups and, depending on the fiber size, by the morphological features, such as high surface area (Seddiqi et al. 2021).

Imparting specific properties to cellulose by suitable functionalizing moieties is an appropriate way to obtain a wide range of materials with multiple and specific activities: catalytic, antibacterial, anti-viral, adhesive, chelating and adsorptive (Coma et al. 2014; Deghles et al. 2019; Dong et al. 2019; Varghese et al. 2019; Muqet et al. 2020; Tang et al. 2021; Deng

et al. 2022). The functionalization can occur through electrostatic adsorption or covalent attachment, which allows a stable link and makes the leaching of the functional group harder (Dufresne 2017). Generally, the covalent linkage on the cellulose surface exploits the hydroxyl groups that can be subjected to several organic reactions, including oxidation, esterification, etherification, activation, and condensation, necessary for the desired functionalization (Credou and Berthelot 2014; Nemeş et al. 2022). Depending on the selected functionalities, the reactions can be carried out by using different solvents, both for the optimization of the functionalization and for the eco-compatibility and health safeness of the synthesis (Heinze and Liebert 2001; Kedzior et al. 2019). The efforts to decrease the impact of such procedures are widely evident in the literature. For instance, Jaekel et al. (2021) developed a sustainable method to extract amino-modified cellulose nanocrystals in an efficient one-step process using reactive eutectic solvents, forming water-dispersible products. In another study, an environmentally friendly method for the esterification of cellulose nanocrystal surface was realized using two non-toxic carboxylic acids, phenylacetic acid and hydrocinnamic acid, which acted both as grafting agents and solvents (Espino-Pérez et al. 2014). Nevertheless, in the case of the functionalization of cellulose with alkyl silyl derivatives, low polarity solvents are often employed, such as toluene, dimethylformamide (DMF) and tetrahydrofuran (THF) (Habibi 2014), when a high degree of substitution and stable dispersion of the starting materials are needed. For instance, aminopropyl silane groups were used as linkers for the preparation of fluorescent cellulose nanocrystals -with potential application in functional papers, sensors and bioimaging- through a grafting procedure involving anhydrous DMF as a solvent (Yang and Pan 2010). Recently, Leong et al. (2019) prepared aminopropyl-cellulose derivatives using non-polar toluene and the materials were used as sorbents to remove rhodamine and crystal violet dyes. These solvents' utilization was due to preventing the oligomerization of silane derivatives that usually occurs in water-based systems, as shown by Robles et al. (2018). In this perspective, ethanol can represent a good compromise to avoid the oligomerization of silane derivatives and, at the same time, to improve the eco-compatibility of the procedure. Indeed, Testa has demonstrated the advantages of

substituting toluene with ethanol in the functionalization of sulfonic propyl silane on silica support (Testa 2021; Testa and La Parola 2021).

Moreover, the interest in waste-derived cellulose (i.e., derived from agricultural scraps, industrial by-products and even waste textiles) is increasing to lower the environmental impact related to the use of virgin plants (Testa and Tummino 2021). The applications of different types of waste cellulose concern a remarkable amount of works where cellulose is studied in several forms and shapes, in many technological fields, as clearly verifiable from the recent literature (Phanthong et al. 2018; Baghel et al. 2021; Noremlyia et al. 2022; Rashid and Dutta 2022; Samrot et al. 2022). In order to give value to waste, some of us (Tummino et al. 2020) have recently used soybean hulls (SBHs) as new sources of chemicals and materials. Soybean hulls are one of the by-products of soybean crushing, and they are mainly constituted of cellulose (29–51%), hemicellulose (10–25%), lignin (1–18%), pectin (4–30%), proteins (11–15%), as demonstrated by different ad hoc reports (Alemdar and Sain 2008; Flauzino Neto et al. 2013; Merci et al. 2015; Ferrer et al. 2016; Debiagi et al. 2020). SBHs have been studied in their pristine form or as a source of carbon for the production of micro-mesoporous adsorbents and biofillers, and also its polysaccharides constituents can find application in different branches of biotechnology (food, medicine, bioremediation, constructions, paper industry, etc.) and biorefinery. Moreover, SBHs are the source of an enzyme, soybean peroxidase, adopted in various applications such as bioremediation and wastewater treatment, biocatalysis, diagnostic tests, therapeutics, and biosensors (Tummino et al. 2020; Lavagna et al. 2021). In a previous work (Tummino et al. 2020), the exhausted soybean hulls obtained after the peroxidase extraction (SBH-A) were recovered and successfully employed as adsorbents in different metal-contaminated waters. The better performances of SBH-A compared to the untreated hulls (SBH-B) were mainly attributed to the enzyme extraction that also acted as a cleaning procedure from some inorganic and organic substances present in the main lignocellulose structure. Thanks to SBH-A cellulose-based composition and the possibility of a double-recovery of a largely produced agricultural scrap, SBH-A-derived cellulose can be eligible as green support for active functionalizing moieties. Indeed, in this study, we used the SBH-A-derived

cellulose to prepare new waste-derived antibacterial materials.

In general, the interest towards novel antimicrobial materials is growing to overcome different problems. Firstly, the phenomenon of antibiotic resistance has to be faced, since bacteria have found their path to survive existing antibiotics, potentially leading to humanitarian and economic crises (Gao et al. 2021). Thus, on the one hand, it is important to develop new drugs and strategies against infections, but, on the other hand, it is necessary to stop or at least contain the pathogen proliferation and spreading, which can occur in different ways, for example, through contaminated surfaces and water (Chaoui et al. 2019; Mahira et al. 2019; Gao et al. 2021; Liguori et al. 2022). It has been reported that the traditional substances used to remove pathogens, like hydrogen peroxide and chlorine-based compounds, are often insufficient to eradicate all the microorganisms (partly due to the evolution of bacteria resistance) and, additionally, cause environmental toxicity issues (Mahira et al. 2019; Srivastav et al. 2020; Kusi et al. 2022). Recently, the application of nanomaterials, mainly based on metal and metal oxide, has been commonly investigated, showing noticeable performances in tackling bacteria action (Mahira et al. 2019; Huang et al. 2020). Nevertheless, the challenge of using and recovering nano-sized particles, with consequent release in the environment and toxicity issues, forces the scientific community to further optimize this kind of materials following the approach of safety-by-design (Musee et al. 2011; Huang et al. 2020). Lastly, one of the newest frontiers in the disinfection field is the preparation of materials starting from sustainable resources, witnessed by several other papers describing bio-based and waste-derived compounds as substrates for antimicrobial functionalities (Muñoz-Bonilla et al. 2019; Al-Tayyar et al. 2020; Ielo et al. 2021; Wu et al. 2022). In the same direction, this work focuses on antibacterial SBH-A waste cellulose after the immobilization of aminopropyl groups. In the last years, in fact, the antibacterial ability of aminated compounds has been reported, from chitin- and chitosan-based (Khatkhat et al. 2019; Tyagi et al. 2019; Li and Zhuang 2020) to amino acid-based systems (Zardini et al. 2012). For instance, regarding NH_2 -containing cellulose, Koshani et al. (2022) prepared aminated

nanocrystalline cellulose from dialdehyde cellulose using ammonia and sodium borohydride and observed a certain bacterial reduction against gram-positive *Listeria monocytogenes* and gram-negative *Salmonella enterica* serotype Typhimurium after 3-h contact. Shao's group (2017) has prepared biocompatible amino alkylsilane-grafted bacterial cellulose membranes with enhanced hydrophobicity features and antibacterial and antifungal properties, effective against *Escherichia coli*, *Staphylococcus aureus*, *Bacillus subtilis* and *Candida albicans*.

Summarizing, in this work, waste cellulose extracted from SBH-A (deproteinized SBHs) was modified by a one-step grafting with 3-aminopropyl triethoxysilane to confer antibacterial properties (Nemeş et al. 2022) and commercial fibrous cellulose derivatives were studied for comparison. The functionalization procedure was optimized by varying the solvent (toluene and ethanol as an eco-compatible alternative), the reaction temperature (strictly connected to the solvent characteristics) and the degree of amino functionalities. Indeed, the overall sustainability pathway consisted of preparing antibacterial materials, progressively decreasing the impact of reaction parameters (choice of waste biomass, greener solvent, lower reaction temperature and reduced reagent amount). Considering the valorization of waste biomass, to the best of our knowledge, this is the first time that this kind of soybean waste has been employed to produce functional materials in view of pathogens' decontamination.

Materials and methods

Extraction of soybean peroxidase

For the extraction of soybean peroxidase (SBP), an established method was used (Calza et al. 2016). Briefly, the soybean seeds were peeled and ground in a mortar (SBH-B), added to phosphate buffer (0.025 M, pH 7) and left under stirring for 2 h at room temperature. Then, the hulls were separated from the solution by filtration with cotton gauze and subjected again to the same treatment until the filtrate responded negatively to the enzymatic activity test for SBP. The hulls were successively dried at room

temperature, cooled by Nitrogen at 77 K and then ground. The final product is labelled SBH-A.

Isolation of cellulose

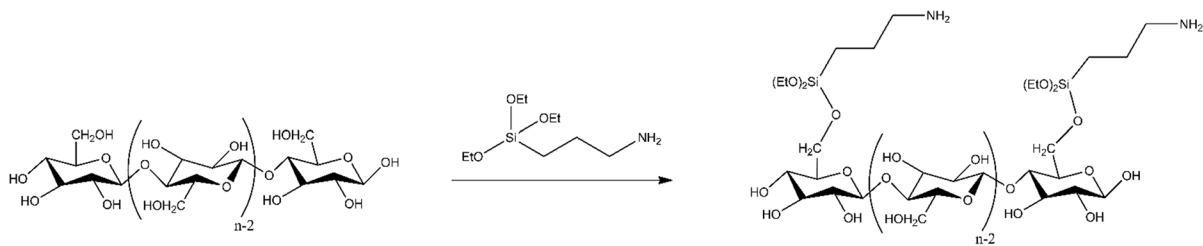
Following the procedure of Sinclair et al. (2018), dried hulls (30 g) were soaked in 300 ml of a NaOH solution (Sigma Aldrich, 2% w/v) and stirred at 80 °C for 2 h. The obtained suspension was filtered on a Buchner funnel (filter Whatman 1) and abundantly washed with deionized water to reach a neutral pH. The pulp was dried in the oven at 60 °C for 4 h. The dried product was treated with an aqueous solution of HCl 1 M (Sigma Aldrich, 2 h at 80 °C) in the ratio 10 g hull-derived product: 100 ml HCl solution, repeating the steps of filtration/washing on Buchner funnel and drying. Lastly, another step with NaOH 2% for 2 h at 80 °C, filtration/washing and drying, was carried out. For comparison, the cellulose isolation procedure was carried out from both SBH-A and untreated hulls (SBH-B).

APTES-cellulose functionalization

In a typical synthesis (Testa et al. 2015; Tummino et al. 2019), a mixture of SBH-A-waste cellulose (W) or commercial fibrous cellulose (F) (cellulose Fibers, medium, Sigma Aldrich) (1 g) and 3-aminopropyl triethoxysilane (APTES, 95%, Sigma-Aldrich) (1.5 or 3 mL) was refluxed in dry ethanol (Sigma Aldrich) or toluene (Sigma Aldrich) (20 mL) during 8 h. The material was filtered *in vacuo* and dried for 2 h at 100 °C. To clarify, Scheme 1 reports the functionalization procedure, whereas Table 1 reports the name of the samples related to the reaction conditions used for their synthesis (solvent type and amount of amino group). The ratios cellulose:APTES are identified as 1:1 and 1:2, when 1.5 and 3 ml of APTES were used, respectively.

Characterization

Elemental analysis (C, H, N, S) was performed on hulls, cellulose and functionalized cellulose with a Thermo Nicolet FlashEA 1112 Series (Waltham, MA, USA). One of the main parameters considered was the Nitrogen content (% wt), as an indicator of NH₂-functionalization. The stability of functionalization for the W-series was verified by washing



Scheme 1 Functionalization reaction of cellulose with 3-aminopropyl triethoxysilane

Table 1 Sample labels and reaction conditions

Sample	Support/functionalizing agent ratio	Solvent
W-E-1	Waste SBH-A Cell/APTES 1:1	Ethanol
W-T-1	Waste SBH-A Cell/APTES 1:1	Toluene
W-E-2	Waste SBH-A Cell/APTES 1:2	Ethanol
W-T-2	Waste SBH-A Cell/APTES 1:2	Toluene
F-E-1	Fibrous commercial Cell/APTES 1:1	Ethanol
F-T-1	Fibrous commercial Cell/APTES 1:1	Toluene
F-E-2	Fibrous commercial Cell/APTES 1:2	Ethanol
F-T-2	Fibrous commercial Cell/APTES 1:2	Toluene

the powders in deionized water (during 3 and 24 h) under stirring; then, the solid was separated and dried to be subjected to elemental analysis and quantify the residual N amount with respect to the initial N value of non-washed samples.

Attenuated total reflectance Fourier transform infrared (ATR-FTIR) spectra were recorded with a Thermo Nicolet iZ10 spectrometer (Milan, Italy) equipped with a Smart Endurance TM (ZnSe crystal) in the range 4000–650 cm^{-1} with 32 scans and 4 cm^{-1} band resolution.

The morphology of samples was examined using an EVO10 Scanning Electron Microscope (Carl Zeiss Microscopy GmbH) with an acceleration voltage of 20 kV. The samples were sputter-coated with a 20 nm-thick gold layer in rarefied argon (20 Pa), using a Quorum SC7620 Sputter Coater.

X-ray diffraction (XRD) analyses were performed using X-ray diffraction (XRD) measurements on a Bruker–Siemens D5000 X-ray powder diffractometer (Bruker AXS, Karlsruhe, Germany) equipped with a Kristalloflex 760 X-ray generator and a curved graphite monochromator using Cu $K\alpha$ radiation (40 kV/30 mA) in reflection mode

(Bragg–Brentano geometry). A proportional counter and 0.05° step sizes in 2θ were used.

The thermal behavior of the samples was investigated by thermogravimetric analysis (TGA) and differential scanning calorimetry (DSC). For TGA analyses (TGA 1 Star System of Mettler Toledo, Schwerzenbach, Switzerland), about 10 mg of sample was heated from room temperature to 100 °C, left at this temperature for 30 min and then heated to 1000 °C at a rate of 10 °C min^{-1} in 30 mL min^{-1} of nitrogen flux. Derivative thermogravimetry (DTG) was used to identify the temperature of maximum mass-loss rates. Differential scanning calorimetry (DSC) was carried out with a DSC calorimeter (Mettler Toledo 821e, Schwerzenbach, Switzerland) calibrated by an indium standard. The calorimeter cell was flushed with 100 ml min^{-1} nitrogen. The run was performed from 30 to 500 °C, at the heating rate of 10 °C min^{-1} and the mass sample was about 5 mg. The data processing was conducted with the STARe Software.

Antibacterial tests

The antimicrobial activity was evaluated according to ASTM E 2149-2013 procedure “Standard test method for determining the antimicrobial activity of immobilized antimicrobial agents under dynamic contact conditions”. This is a quantitative method performed under dynamic contact conditions. The bacteria were *Escherichia coli* ATCC 11229 (gram-negative) and *Staphylococcus aureus* ATCC 6538 (gram-positive).

The bacteria were grown in a proper nutrient broth (Buffered peptone water for microbiology, VWR Chemicals) for 24 h at 37 °C. The bacteria concentration was measured with a spectrophotometer and diluted into a sterile buffer to give a $1.5\text{--}3.0 \times 10^5$ CFU/ml working dilution. This

bacterial inoculum was put in contact with the antibacterial agent (cellulose powder) under shaking at room temperature for 1 h (the standard cellulose/inoculum ratio was 1 g/50 ml). After this time, 1 ml of inoculum was diluted 1000 times and plated in Petri dishes with Yeast Extract Agar (Sigma Aldrich). The Petri dishes were incubated 24 h at 37 °C and, then, the surviving bacteria colonies were counted and compared to the initial bacteria concentration of the inoculum to calculate the % bacterial reduction using this equation (Eq. 1).

$$\text{Reduction}(\%) = \frac{(A - B) \times 100}{A} \quad (1)$$

where A = number of viable microorganisms before treatment, B = number of viable microorganisms after treatment. When necessary, the antibacterial agent/inoculum ratio was varied: these cases are underlined in the Results and Discussion section.

The antimicrobial effect of amino group leaching in solution was investigated by putting the cellulose powder in contact with the sterile buffer (ratio 1 g/50 ml). After one hour, the liquid phase was separated from the deposited solid (that was then left to dry) and both portions were independently subjected to the antibacterial tests (towards *E. coli*), following the ASTM E 2149-2013 procedure.

Results and discussion

Isolation of cellulose from SBH-A and SBH-B

First, it is worth underlining that the cellulose isolation was performed by following a conventional chemical method: the combination of both acid and alkali treatments for obtaining soybean hull cellulose

has been robustly demonstrated as effective in the removal of hemicellulose, lignin and minor components (Alemdar and Sain 2008; Ferrer et al. 2016; Sinclair et al. 2018; Iglesias et al. 2021).

In this work, cellulose was isolated from SBH-A and SBH-B in the form of powders with a light brown color, indicating the presence of a small portion of chromophore-rich compounds left from the hulls' lignocellulosic matrix. In Supplementary Information (Fig. S1), the infrared spectra of the solids recovered at different isolation steps (alkaline-acid-alkaline) and the filtrated part after the first NaOH treatment are reported as proves of the progressive efficiency of the cellulose isolation procedure. An overall yield of $36 \pm 1\%$ of final cellulose product (quantified with respect to the initial hulls' weight) was obtained by SBH-A, whereas for SBH-B, the yield was $29 \pm 3\%$. This difference can be attributed to the higher cleanliness of SBH-A, which, in turn, did not present filter clogging problems during the isolation and allowed an easier recovery of the material (contrarily to what happened with SBH-B). Indeed, as demonstrated in the previous work (Tummino et al. 2020), the SBP extraction in phosphate buffer served as a preliminary purification of the lignocellulosic backbone from minor organic components (especially the peptidic portion) and metals (such as iron, aluminum and manganese).

The elemental compositions (C, H, N, S) of SBH-A, SBH-B, the derived waste celluloses and the commercial reference sample (F) are reported in Table 2. The presence of N in both soybean hull samples and SBH-B cellulose is reasonably an index of peptide/protein content, following the order: SBH-A-derived and F-cellulose < SBH-B cellulose << SBH-A < SBH-B. The C/H ratios of both SBH-derived cellulose specimens are in good agreement with the reference F-cellulose, with the

Table 2 Elemental composition of different SBHs and derived celluloses

Element	Samples				
	SBH-A	SBH-B	Cellulose from SBH-A	Cellulose from SBH-B	F-cellulose
C (wt%)	41.27 ± 0.16	41.37 ± 0.08	42.62 ± 0.03	42.74 ± 0.03	42.00 ± 0.10
H (wt%)	5.94 ± 0.07	6.09 ± 0.05	6.07 ± 0.04	6.16 ± 0.04	6.03 ± 0.08
N (wt%)	1.28 ± 0.01	1.50 ± 0.06	0	0.07 ± 0.05	0
S (wt%)	0	0	0	0	0
C/H	6.95	6.79	7.02	6.94	6.97

theoretical ratio based on the cellulose molecular structure and with other studies reporting cellulose elemental composition (Carrier et al. 2011; Liang et al. 2018; Zheng et al. 2021). The same parameter, analyzed for the hulls SBH-A and SBH-B, is not so far from the previous quantifications, demonstrating that the original biomass contains a limited amount of lignin (as already found in the literature Merci et al. 2015), which, otherwise, would have significantly increased the C/H values (Cagnon et al. 2009; Muley et al. 2016; Zhang et al. 2021).

For a more exhaustive characterization of SBH-A and SBH-B, reference should be made to (Tummino et al. 2020), whereas from the comparison of other physical–chemical features of the final cellulosic products, evaluated by ATR-FTIR, SEM and DSC (data not shown), it emerged that the two starting SBH precursors originated very similar products. The only slight differences were revealed by ATR-FTIR of SBH-B-derived cellulose, where small signals related to protein content and/or aromatic $-C=C-$ stretching (around 1540 cm^{-1} and 810 cm^{-1}) are assignable to residual proteins and hemicellulose (Jungnikl et al. 2008; Hudson-Mcaulay et al. 2020; Tummino et al. 2020). SBH-A was then chosen as the waste cellulose source for further functionalization.

Characterization of materials

The effectivity of the APTES functionalization on waste SBH-A cellulose (W) was ascertained by the quantification of Nitrogen in the samples through Elemental Analysis (see Fig. 1a). The same test was carried out also on the commercial fibrous cellulose (F), representing the pure reference material. Since the bare commercial sample and the waste cellulose are devoid of Nitrogen, the results related to N amount are not inserted in the comparative graph. As shown in Fig. 1a, the N amount was generally higher for W-samples (about 0.6%) with respect to the F-derivatives and, among the F-samples, the syntheses carried out in the presence of ethanol led to a higher functionalization efficiency. Moreover, the obtained N (wt%) values are substantially independent of the cellulose:APTES ratios, indicating that the functionalization reached a maximum with respect to the available cellulose sites. Unexpectedly, W-T-1 behavior stands out with respect to the other similar samples, presenting a N content of *ca.* 0.9%. For this

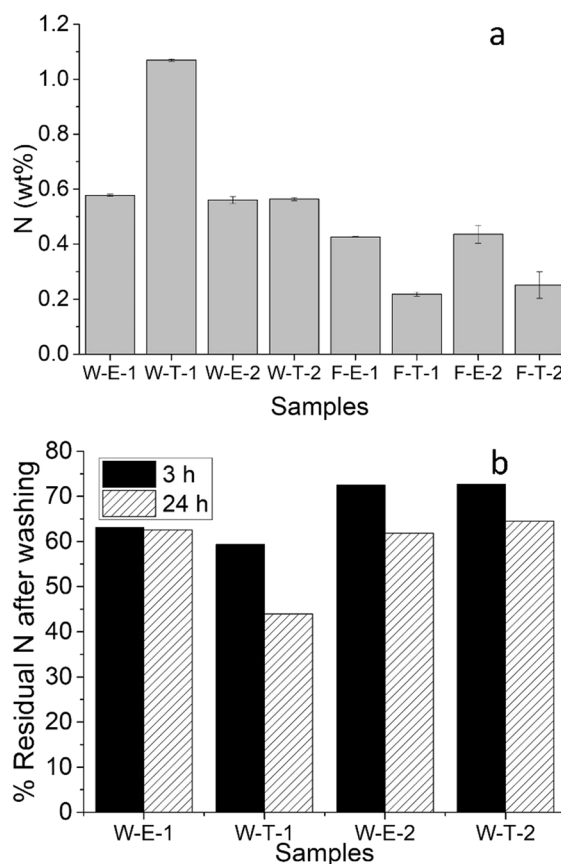


Fig. 1 **a** N content (wt%) from elemental analysis; **b** percentage of residual nitrogen after washing procedure

reason, the stability of the materials and the leaching of the amino groups in waste cellulose derivatives were studied and the results are reported in Fig. 1b. After 24 h of washing, the N loss related to W-T-1 was the most pronounced indicating that a significant fraction of the amino groups was only physisorbed or weakly attached to the cellulose surface. For all the other samples, after 24 h, a similar degree of residual N percentage (around 60%) was reached. The same tests carried out for comparison on F-cellulose derivatives showed an average loss of 40% after 3 h, and up to 60% after 24 h.

The data about functionalization degree and stability seem to primarily indicate higher effectiveness of the functionalization procedure in the presence of ethanol as a solvent, which is eco-compatible and also works at a lower refluxing temperature ($77\text{ }^{\circ}\text{C}$ for ethanol vs. $110\text{ }^{\circ}\text{C}$ for toluene). Indeed, although ethanol is a poor solvent for semicrystalline cellulose

because it cannot decrystallize and well disentangle cellulose chains (Naz et al. 2016; Ghasemi et al. 2017), it can promote, due to its polarity, the breakage of some hydrogen bonding among the cellulose chains (Robles et al. 2018), increasing the availability of hydroxyl groups for the functionalization process (Juntaro et al. 2012; Naz et al. 2016). Secondly, a possible explanation of the higher degree (and stability) of functionalization on SBH-A waste cellulose with respect to the commercial one is related to the alkaline treatment suffered during its isolation. In fact, such treatment acted by disrupting the $-OH$ bonding in the fiber structure, producing ionization and leading to an alkoxide (Fiber- O^-). After the abundant washing cycles performed on our samples, most of the form Fiber-OH has been restored, but such a strong procedure may have left some changes in the chemical reactivity (Stepanova and Korzhikova-Vlakh 2022).

ATR-FTIR measurements for all the analyzed samples mainly showed the typical signals of cellulose (see the spectra of some selected powders with the related attributions in Supplementary Information and Figure S2) (Yang et al. 2007, 2017). The sufficient degree of cellulose isolation from SBH-A at the expense of other components is confirmed by the absence of the peak at 1745 cm^{-1} , which is related to either the acetyl and uronic ester groups of the hemicelluloses or the ester linkage of the carboxylic group of the ferulic and p-coumaric acids of lignin and/or hemicellulose (Camiscia et al. 2018). This peak, indeed, is visible in Fig. S1, in the spectra of SBH-A and SBH-A after HCl treatment. For the functionalized samples, the shoulder at about 1560 cm^{-1} can be ascribed to the N-H bending of primary amines (Sheltami et al. 2015; Zhang et al. 2016) and can be assumed as another proof of APTES attachment.

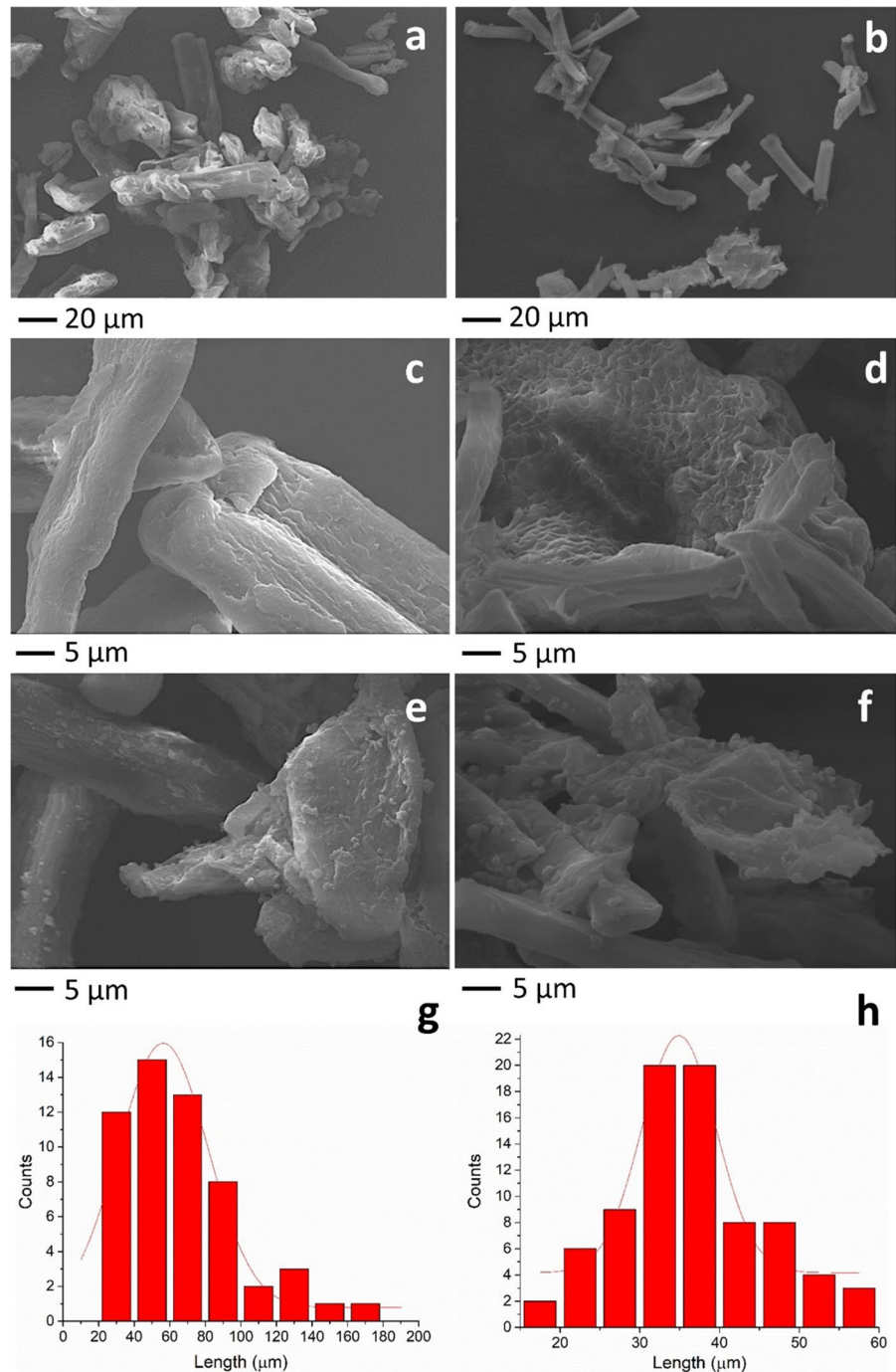
In order to study the morphology of celluloses (F and W) and the corresponding amino samples, SEM analysis was carried out (see Fig. 2). F-cellulose and its derivatives exhibited both fibers and some aggregates (Fig. 2a, c, e). In all SBH-A celluloses (Fig. 2b, d, f), some cemented regions could be distinguished, presumably due to residual hemicellulose, lignin and other minor components around the fiber-bundles (Alemdar and Sain 2008) (see specifically Fig. 2d), whose presence can also be witnessed by the light brown color of the W-cellulose-based powders. Moreover, it is possible to assert that no morphological

changes were evidenced after the APTES immobilization, showing the negligible influence of the functionalization procedure on the morphology of the considered samples. The variation of functionalization parameters had, as a sole visible effect, the presence of some round-shaped impurities in F-T-1 and W-T-1 (Fig. 2e, f). In particular, W-T-1 has already been mentioned for its out-of-range N-content, which can be correlated with the presence of physisorbed aminopropyl silane on the fiber surface. As a representative dimensional parameter, the distribution of fiber lengths, fitted by a Gaussian function, displayed a narrower range of lengths for W-celluloses that were also shorter than the reference F-celluloses. Actually, such distribution values are centered at $56 \pm 3\text{ }\mu\text{m}$ for commercial cellulose-derived samples and $35 \pm 1\text{ }\mu\text{m}$ for soybean hulls-derived ones (Fig. 2g, h).

The X-ray diffractograms of all the considered samples were very similar among them. They were consistent with the typical pattern of crystalline cellulose type I β (monoclinic) (Park et al. 2010), exhibiting the principal peaks at 14.5° , 16.5° and 22.5° 2θ , which are attributed to the planes (1 -1 0), (1 1 0), and (2 0 0) (French 2014; Gong et al. 2017), respectively (Fig. 3). According to Alemdar and Sain (2008), the hydrogen bonds between cellulose molecules are arranged in ordered systems (crystallites) with crystal-like properties, interrupted by disordered (amorphous) regions. In this work, no evidence of structural changes caused by amino-functionalization was detected in the case of the F-series nor in the W-series. Overall, both XRD and SEM results obtained in this study are in good agreement with the literature (Flauzino Neto et al. 2013; Merci et al. 2015).

Figure 4 displays the main outcomes of thermal analyses (TGA and DSC). Figure 4a reports some representative TGA thermograms. All the materials showed similar trends of thermal degradation, except around $230\text{--}400\text{ }^\circ\text{C}$ (see the comment on DTG curves for the explanation). The remaining residues at $1000\text{ }^\circ\text{C}$ corresponded to 8 wt% for F-cellulose, 12 wt% for W-cellulose and 13–21 wt% for aminated celluloses. These values are in line with the presence of small amounts of impurities within W-cellulose and the introduction of APTES groups in the functionalized samples, which increased the quantity of residual mass (char and ashes (Azubuike and Okhamafe 2012; Khanjanzadeh et al. 2018)).

Fig. 2 SEM images of various samples at different magnifications (on the left F-series and on the right W-series are reported), precisely **a** bare F-cellulose, **b** bare W-cellulose, **c** F-E-1, **d** W-E-1, **e** F-T-1, **f** W-T-1. Graphs **g** and **h** are the length distributions for F- and W-samples' series, respectively



From the examination of DTG curves (see examples in Fig. 4b), a certain temperature shift of the peak that indicates the maximum degradation rate (T_{mdr}) was visible. In particular, such peaks were centered at 345 °C for F-cellulose, at about 352 °C for F-T-1

and F-T-2, and around 364 °C for W-cellulose, W-E-1, W-E-2, W-T-2, F-E-1 and F-E-2.

In general, the quantity of the attached APTES (see Fig. 1a) and the presence of residual impurities in SBH-A-derived samples are the most probable factors

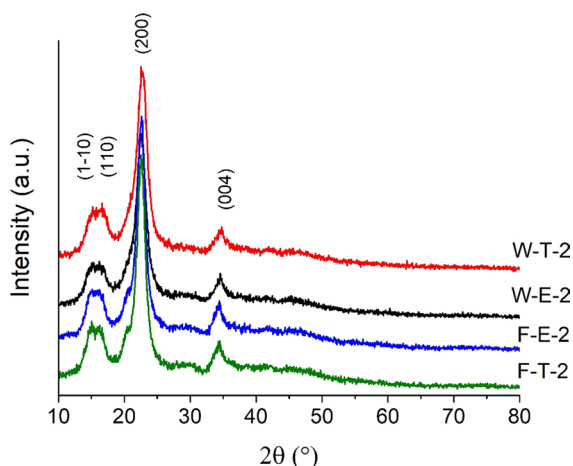


Fig. 3 X-ray patterns for selected samples, with the indication of the main lattice planes

that influenced the major thermal degradation phenomenon. For instance, beyond the bare F-cellulose, both F-T-1 and F-T-2 (prepared from commercial cellulose with toluene) showed the minimum presence of amino groups and, concurrently, the lowest T_{mdr} . It is also worth noting that, for the samples with the best thermal stability (namely highest T_{mdr}), the DTG curves manifested a non-flat trend in the range 225–300 °C, suggesting that some initial events could have formed a protective and stabilizing layer. Two distinct stages characterize cellulose decomposition: slow endothermic dehydration of the hydroxyl groups to form anhydro-cellulose (at about 200–280 °C) and a faster unzipping of the remaining cellulose polymer chain at temperatures above 280 °C, yielding a complex mixture of char residues and gas (Durkin et al. 2019). It has already been reported that APTES and similes can improve cellulose thermal properties due to the possibility of binding two or more cellulosic hydroxyl groups during the functionalization reaction (Voicu and Thakur 2021) and the consequent crosslinking effect (Khanjanzadeh et al. 2018; Bessa et al. 2021). Moreover, the APTES stabilizing mechanism in pyrolysis may involve the initial formation of an insulating siloxane coating on the cellulose surface that acts as a heat transfer barrier and delays the unzipping of the biopolymer (Durkin et al. 2019). Nevertheless, in particular conditions, this process can be hindered: Neves et al. (2020) claimed that the 3-aminopropyl triethoxysilane modification of

microcrystalline cellulose caused a reduction in crystallinity which facilitated the heat diffusion along the sample and decreased the heat resistance.

The other significant parameter affecting thermal properties was the use of W-cellulose. In this case, the primary degradation step (250–300 °C) can be imputable to the behavior of residual hemicellulose components such as xylan and glucomannan (Garcia-Maraver et al. 2013; Wang et al. 2020). On the other hand, the delay of the principal phenomenon could be governed by the presence of lignin and other polyphenolic compounds (rich in aromatic groups and ether carbon bonds), which improved the thermal stability, as suggested by several studies (Garcia-Maraver et al. 2013; Jiang et al. 2019; Zhang et al. 2019).

The T_{mdr} shift tendency shown by DTG coincides with that found for DSC outputs, as observable in Fig. 4d and its correlation to Fig. 4b. In this regard, Fig. 4c (yellow histogram, on the bottom) globally reports the temperatures of DSC peaks in the range of 300–400 °C, implying an overall endothermic phenomenon. In general, the thermal degradation properties of the amino-silylated and waste-derived materials presented in this work resulted in a sufficient stability level to eventually support traditional thermal sterilization treatments, which are generally required, for instance, in medical applications (Chantreau et al. 2019).

The effects of the cellulosic support and the type of solvent can also be discussed by looking at the DSC peak area integrations for the different samples, representing the enthalpy (ΔH) of the heat-driven transformation (Fig. 4c, grey histogram, on the top). It is possible to recognize a complementarity between the temperature of the DSC peak (proportional to T_{mdr} and, thus, stability) and its integration. For example, F-cellulose, F-T-1 and F-T-2 results showed the highest ΔH , which was in opposition to the T-trend. In particular, the combination of both W-cellulose and ethanol most significantly decreased the ΔH value. To explain this outcome, on the one hand, we can assume that the thermal phenomena are distributed along a broader range of temperatures in analogy to TGA, due to APTES and leftover lignocellulosic compounds, decreasing the energy involved in the principal transformation. On the other hand, it is necessary to deepen the meaning of that DSC peak for cellulose: it corresponds to a complex overlapping of different events, namely the fusion of its crystalline

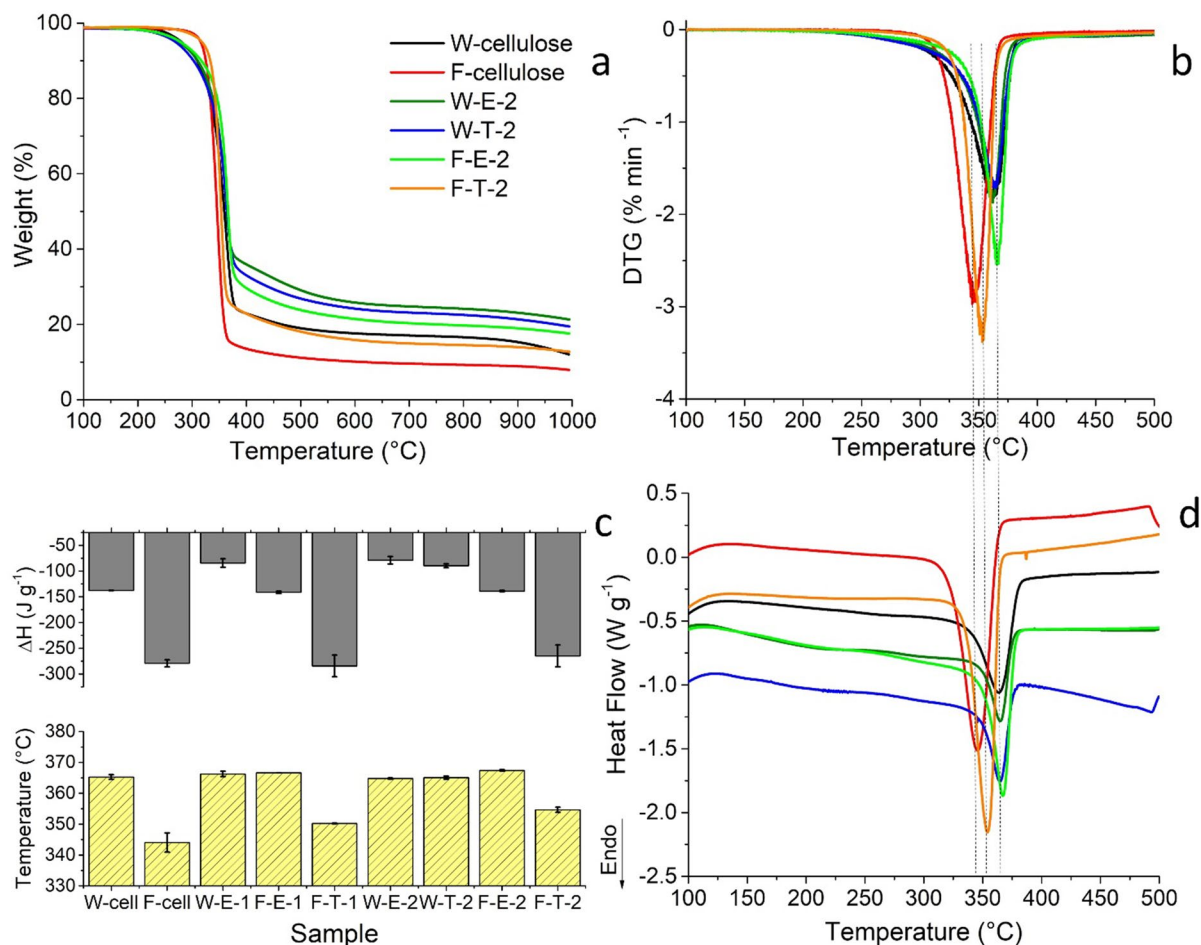


Fig. 4 **a** TGA thermograms of selected samples; **b** DTG curves related to samples in (a); **c** histograms reporting the temperatures of the DSC peaks and the values of the areas under the peaks (ΔH); **d** DSC curves related to samples in (a, b)

part (endothermic) and the depolymerization (exothermic) (Morán et al. 2008; Rosa et al. 2012; Helmiyati and Yulianti 2014). The predominance of one over the other event depends on various parameters, such as molecular weight, amorphous content, crystallite sizes, etc. (Rosa et al. 2012). In our study, both the intrinsic W-cellulose characteristics and ethanol interaction with cellulose may have influenced those features, also considering the already discussed results regarding the different functionalization efficiencies, due to solvent and cellulose type reactivity.

For the sake of clarity, TGA and DSC results for the sample W-T-1 were not reported, since its level of uncleanness seriously affected the analyses. In particular, its thermal degradation pathway was

more similar to F-T-1 and F-T-2 than all the other W-cellulose samples. Regarding DSC, W-T-1 did not show the endothermic peak, leaving only the exothermic component and, thereby, confirming a certain instability.

Antibacterial activity

After the optimization of the synthetic procedure and the deep characterization of the materials, it was possible to study the antibacterial properties of functionalized waste cellulose. The antibacterial test outcomes, obtained following the ASTM procedure using the cellulose/inoculum ratio as 1 g/50 ml, evidenced that all the functionalized samples reached 100% bacterial reduction after 1 h-contact for both the

Table 3 *E. coli* reduction (%) obtained by decreasing the amount of functionalized cellulose in contact with the bacterial inoculum

Sample	Bacterial reduction (%)
Functionalized W-samples in standard conditions	100
W-E-1 (1:250)	99.7
W-E-1 (1:5 000)	96.8
W-E-1 (1:10 000)	96.8
W-T-1 (1:500)	100
W-T-1 (1:10 000)	97.6
W-E-2 (1:250)	99.7
W-E-2 (1:500)	99.7
W-E-2 (1:10 000)	93.3
W-T-2 (1:250)	100
W-T-2 (1:500)	100
W-T-2 (1:10 000)	97.4

The ratios in brackets represent the number of folds in which the cellulose amount was diminished with respect to standard tests

bacterial strains (*Staphylococcus aureus* and *Escherichia coli*). In order to underline eventual differences, the amount of functionalized cellulose was decreased in ad hoc trials with *Escherichia coli*, and the related results are summarized in Table 3, showing, again, a superior antibacterial activity. The tests were made in duplicate and the error was lower than 1%, except in the case of W-E-2, for which the error was estimated as 5%, mainly due to experimental fluctuations than specific events with detrimental effects.

Previous studies on other antibacterial cellulosic materials tested with the same ASTM method, for a better comparison, showed as the most exploited functionalities have involved positively-charged N-based species (Hassanpour et al. 2017, 2018; Tyagi et al. 2019; Sperandeo et al. 2020). For instance, quaternium silane salt (Hassanpour et al. 2017) and phenanthridinium silane salt (Hassanpour et al. 2018) onto nanofibrillated cellulose exhibited a certain antimicrobial activity, with a predominant effect on gram-negative or gram-positive bacteria depending on the functionalizing salt. Sperandeo et al. (2020) optimized the functionalization of microcrystalline cellulose powder with two peptides (lasioglossin-III and TBKKG6A) able to show antimicrobial activity at low concentrations. The peptide-modified cellulose

obtained a 100% bacterial reduction towards *E. coli* at the concentration ratios cellulose/inoculum 1 g: 50 ml in the case of lasioglossin-III (as in our first standard tests) and 2.5 g: 50 ml in the case of TBKKG6A (Sperandeo et al. 2020).

Since a portion of amino groups was found to be released in aqueous media (see Fig. 1b), further tests were conducted to check whether the antibacterial activity of functionalized W-cellulose against *E. coli* was maintained after the partial leaching of amino groups. The results showed that all the recovered materials (W-E-1, W-T-1, W-E-2 and W-T-2) still led to complete bacteria removal. For the sake of accuracy, also the solution put in contact with the cellulosic powder showed antibacterial activity, indicating that also the released amino groups undertook an action in the homogeneous phase representing other points of attack against pathogens, as occurs in the case of biocide-releasing polymers (Siedenbiedel and Tiller 2012). Although this kind of activity has to be specifically investigated to assess its environmental impact, in the first instance, we can say that (i) APTES is considered a relatively safe reactant (Shi et al. 2011; Esparza-González et al. 2016; Shao et al. 2017; Khanjanzadeh et al. 2018) and (ii) the quantity released in antibacterial tests with the decreased (1: 10,000) cellulose/inoculum ratio would be in the magnitude order of ppb.

Both non-functionalized celluloses (commercial and from SBH-A), used as references in standard tests, did not show any antibacterial activity against *S. aureus* (gram-positive) and, analogously, bare F-cellulose was practically inactive towards *E. coli* (gram-negative) with 15% bacterial reduction. This result is not surprising since it is known that cellulose does not possess inherent antibacterial activity (Khattak et al. 2019; Rashki et al. 2021). Nevertheless, bare W-cellulose reached a 52% bacterial reduction in the presence of *E. coli*. Even though this evidence does not allow us to consider soybean hull-derived cellulose as an antibacterial in the strict sense, it deserves some considerations. First, since the pH of the suspensions of W-cellulose in distilled water was 7 and no particular contaminants (e.g., salt crystals) were detected by a deep analysis of the samples by SEM, we can rule out the presence of non-removed excess inorganic chemicals (such as NaOH, NaCl) used or formed in the cellulose extraction process and which could have any significant antibacterial activity. Second, soybean

seeds are recognized as sustainable sources of various phytochemicals, such as isoflavones and other polyphenols (Villalobos et al. 2016; Abutheraa et al. 2017; Hosseini Chaleshtori et al. 2017; Carneiro et al. 2020; Nile et al. 2022). In different studies, the main isoflavones identified in soybean hulls and okara (residual portion obtained after filtering the water-soluble fraction during the production of soymilk or soybean curd (Nile et al. 2020)) are daidzein, daidzin, genistein, genistin, glycitin, and glycitein (Nile et al. 2022). Other compounds are phenolic acids (such as gallic, ferulic, syringic) and flavonoids (such as (+)-catechin, (-)-epicatechin and quercetin) (Cabezudo et al. 2021). The amount/kinds of extracts reported are influenced by the seed varieties (e.g., yellow, brown, dark brown, black) (Abutheraa et al. 2017) and their extraction treatment method (Cabezudo et al. 2021; Nile et al. 2022). Another distinction is related to the linkage of these molecules to the cell wall structural components (Zhang et al. 2020). Free-form phenolics are directly released in water/organic solvent mixtures, while conjugated (esterified) and insoluble-bound forms, which are considered to be bound to oligosaccharides, peptides or polysaccharides, can be traditionally released after acidic or alkaline hydrolysis (Niño-Medina et al. 2017) or, as an alternative, by enzymatic methods (Cabezudo et al. 2021). All these compounds are well-known for beneficial properties like anti-cancerous, antioxidant, anti-inflammatory, anti-osteoporosis and antimicrobial ones (Villalobos et al. 2016). Lignin itself, with its polyphenolic structure, is considered antimicrobial and antioxidant (Alzagameem et al. 2019). The antimicrobial effect of these substances is related to the disruption of the microorganism plasma membrane and is influenced by polyphenol hydrophobic and amphiphilic character, the size and type of alkyl groups, the molecular weight, the presence of acetate and aldehydes groups and, in particular, by the amount and the position of OH groups (Lopez-Romero et al. 2015; Bouarab-Chibane et al. 2019; Guimarães et al. 2019; Álvarez-Martínez et al. 2021). The hydroxyl group accumulation alters the hydrophobicity and surface charge of the microorganism membrane, causing lipid segregation, local ruptures, pore formation and leakage, among other disruptive effects (Bouarab-Chibane et al. 2019; Álvarez-Martínez et al. 2021). Regarding our results, despite the strong acid/basic treatment that SBH-A underwent

during cellulose isolation (with the removal of most of the non-cellulosic matter, as confirmed by FT-IR), some residual minor components, derived from the original matrix and detected by TGA and microscopy, could have maintained a portion of active phenolics, presumably the insoluble ones which were freed by the hydrolytic process (Niño-Medina et al. 2017; Zhang et al. 2020). A previous study has pointed out that, even after pulping and bleaching stages occurring during cellulose separation, a minimal amount of chromophore compounds (including quinoid and other aromatics) can be left in the ppm-ppb range and are still visible as off-white or yellowish coloration (Rosenau et al. 2005). As a matter of fact, in a more recent paper, these substances have also been detected in lignin-free cellulosic materials and have been considered as consequences of oxidative damage to the cellulose and hemicelluloses (Korntner et al. 2015). Therefore, in this work, a compresence of different types of substances can be hypothesized.

Another noteworthy aspect concerns the activity of bare W-cellulose only towards a gram-negative bacterium. It has been ascertained that there are differences in the susceptibility to antimicrobials between gram-positive and gram-negative bacteria due to their cell envelope structure and composition (Lopez-Romero et al. 2015; Luo et al. 2022). The gram-negative bacteria cell wall is constituted by a thin peptidoglycan layer adjacent to the cytoplasmic membrane and an outer membrane composed of phospholipids and lipopolysaccharides. The passage through the outer membrane is regulated by the presence of hydrophilic channels (porins) (Guimarães et al. 2019), which can exclude the entry of hydrophobic substances, although exceptions have been demonstrated (Lopez-Romero et al. 2015; Lu et al. 2016; Guimarães et al. 2019; Luo et al. 2022). On the other hand, gram-positive bacteria lack the outer membrane, but the cell wall is formed by a thicker peptidoglycan layer that confers rigidity to cells and makes it difficult to penetrate by some antimicrobials. Another characteristic that plays a fundamental role in antimicrobial effectiveness is the charge of the cell surfaces, which, under physiological conditions, usually is negative due to the presence of anionic groups in the membrane (e.g., carboxyl and phosphate) (Lopez-Romero et al. 2015). In particular, regarding the charge interaction between bacteria and antimicrobial agents, Maruthapandi et al. (2022) reported

that a negative zeta potential characterizes both gram-positive bacteria (prevailing polysaccharides) and gram-negative bacteria (teichoic acids bonded to the peptidoglycan layer). For instance, the average zeta potential observed for *S. aureus* is -35.6 mV and for *E. coli* is -44.2 mV. Therefore, cationic antimicrobial agents, such as amino-based compounds, trigger the inactivation pathway from the adhesion and puncture to the negatively-charged membrane of bacteria (Arora and Mishra 2018; Luo et al. 2022), leading to its destabilization and eventually inducing microorganisms' death. Given these premises, if we consider only the cellulosic component of the isolated product from SBH-A, we cannot point out either peculiarity in the surface charge of bare W-cellulose (negative) (Camiscia et al. 2018; Tummino et al. 2020; Luo et al. 2022) or its changes in hydrophilicity with respect to the reference cellulose (F), only on the basis of the type of acid–base treatment employed for the isolation and the results of chemical analyses. What could occur is the role of W-cellulose as a passive polymeric layer, which was able to prevent the adhesion of bacteria by decreasing the protein adsorption on its surface, thereby repelling the bacteria without actively interacting with it (Arora and Mishra 2018). Moreover, even assuming that residual polyphenols can play a role in antimicrobial action, several reports state that different gram-positive and negative strains are diversely susceptible to soybean-derived isoflavones and phenolic compounds (Villalobos et al. 2016; Abutheraa et al. 2017; Hosseini Chaleshtori et al. 2017), leaving the question open with a non-unique explanation of the phenomenon.

Conclusions and perspectives

Waste cellulose, extracted from deproteinized soybean hulls' biomass by an acid–base treatment, was functionalized with aminopropyl groups to impart antibacterial properties. After the optimization of the synthesis, the aminopropyl groups were grafted in refluxing ethanol by a basically simple one-step procedure obtaining new materials with excellent antibacterial performances.

In more detail, the use of sustainable ethanol resulted in a better functionalization efficiency than toluene, due to higher polar interactions with cellulose during the reaction and, thus, in better stability

of the material, as assessed by thermal analyses. The use of soybean hulls'-derived cellulose compared with commercial cellulose evidenced the effects of impurities derived from the original lignocellulosic matrix, although in small quantities non-detected by FT-IR. These compounds are hypothesized to be unremoved hemicellulose, lignin and other aromatic compounds, freed by the hydrolytic isolation of cellulose. Their beneficial influence was, again, reflected in functionalization efficiency and thermal stability, but interestingly also in the antibacterial properties of W-cellulose. Summarizing, the type of biomass from which cellulose originated, the extraction strategy, and, in addition, the solvent used for cellulose modification play very crucial roles in the final characteristics and applications. In this study, the best performances were achieved using waste cellulose reacting in ethanol with the loading ratio cellulose: APTES 1:1, which represents, at the same time, the most active and stable sample obtained by the greenest combination of processing parameters. Moreover, from the comparison with the literature, we can say that the main advantages of the amino-modified SBH-derived materials examined in the present work are the exceptional and fast bacterial reduction, also in small concentrations, towards both gram-positive and gram-negative bacteria.

Concerning future perspectives, it will be important to increase the sustainability of cellulose isolation with greener chemicals, enzymatic procedures, or physical treatments (Radotić and Mičić 2016; Dufresne 2017; Rana et al. 2021; Gao et al. 2022; Pradhan et al. 2022), and evaluate their effect on the final aminated materials. Additionally, the study of residual compounds in SBH-cellulose, among which the polyphenolic phytochemicals, deserves specific investigations.

Finally, the functionalization approach studied in this work can be considered a starting point for developing other materials based on cellulose (especially waste cellulose) which can be employed in different sectors (i.e., antibacterial surfaces, textiles, etc.). In powdery form, APTES-waste cellulose can be used in formulation with other materials, such as polymeric blends and composites. Moreover, it can be applied as a powder filter for water depuration goals, in particular, during the first steps of water treatments, in which preliminary enhancement of wastewater quality and disinfection occur. This circumstance is highly

desirable in the presence of high pathogen contamination levels and antibiotic resistance risk, as an alternative to traditional and sometimes ineffective chlorinated and peroxide-based processes.

Acknowledgments We thank Dr. Francesca Deganello of CNR-ISMN for her support in the XRD interpretation.

Author contributions All authors contributed to the study conception and design. Material preparation was performed by MLT1, MLT2 and EL, data collection and analysis was performed by MLT1, CC, VLaP, CV, PB. The first draft of the manuscript was written by Maria Laura Tummino and all authors commented on previous versions of the manuscript. All authors read and approved the final manuscript.

Funding The authors declare that no funds, grants, or other support were received during the preparation of this manuscript.

Data availability All data supporting the findings of this study are available within the article.

Declarations

Conflict of interest The authors have no relevant financial or non-financial interests to disclose.

Consent for publication The authors agreed with the content and all gave explicit consent to submit and publish the results presented in the article.

Ethics approval and consent to participate This article does not contain any studies with human participants or animals performed by any of the authors. The authors claim the compliance with the ethical standards.

Open Access This article is licensed under a Creative Commons Attribution 4.0 International License, which permits use, sharing, adaptation, distribution and reproduction in any medium or format, as long as you give appropriate credit to the original author(s) and the source, provide a link to the Creative Commons licence, and indicate if changes were made. The images or other third party material in this article are included in the article's Creative Commons licence, unless indicated otherwise in a credit line to the material. If material is not included in the article's Creative Commons licence and your intended use is not permitted by statutory regulation or exceeds the permitted use, you will need to obtain permission directly from the copyright holder. To view a copy of this licence, visit <http://creativecommons.org/licenses/by/4.0/>.

References

- Abutheraa R, Hettiarachchy N, Kumar-Phillips G et al (2017) Antimicrobial activities of phenolic extracts derived from seed coats of selected soybean varieties. *J Food Sci* 82:731–737. <https://doi.org/10.1111/1750-3841.13644>
- Alemdar A, Sain M (2008) Isolation and characterization of nanofibers from agricultural residues-wheat straw and soy hulls. *Bioresour Technol* 99:1664–1671. <https://doi.org/10.1016/j.biortech.2007.04.029>
- Al-Tayyar NA, Youssef AM, Al-hindi R (2020) Antimicrobial food packaging based on sustainable bio-based materials for reducing foodborne pathogens: a review. *Food Chem* 310:125915. <https://doi.org/10.1016/j.foodchem.2019.125915>
- Álvarez-Martínez FJ, Barrajón-Catalán E, Herranz-López M, Micol V (2021) Antibacterial plant compounds, extracts and essential oils: an updated review on their effects and putative mechanisms of action. *Phytomedicine* 90:153626. <https://doi.org/10.1016/j.phymed.2021.153626>
- Alzagameem A, Klein SE, Bergs M et al (2019) Antimicrobial activity of lignin and lignin-derived cellulose and chitosan composites against selected pathogenic and spoilage microorganisms. *Polymers (Basel)* 11:670. <https://doi.org/10.3390/polym11040670>
- Arora A, Mishra A (2018) Antibacterial polymers: a mini review. *Mater Today Proc* 5:17156–17161. <https://doi.org/10.1016/j.matpr.2018.04.124>
- Azubuiké CP, Okhamafe AO (2012) Physicochemical, spectroscopic and thermal properties of microcrystalline cellulose derived from corn cobs. *Int J Recycl Org Waste Agric* 1:9. <https://doi.org/10.1186/2251-7715-1-9>
- Baghel RS, Reddy CRK, Singh RP (2021) Seaweed-based cellulose: applications, and future perspectives. *Carbohydr Polym* 267:118241. <https://doi.org/10.1016/j.carbpol.2021.118241>
- Bano S, Sultana S, Sabir S, Khan MZ (2021) Advanced application of green materials in environmental remediation. In: *Applications of advanced green materials*, ed. Shakeel A, Woodhead Publishing in Materials, pp 481–502. <https://doi.org/10.1016/B978-0-12-820484-9.00019-2>
- Bessa W, Tarchoun AF, Trache D, Derradji M (2021) Preparation of amino-functionalized microcrystalline cellulose from *Arundo Donax* L. and its effect on the curing behavior of bisphenol A-based benzoxazine. *Thermochim Acta* 698:178882. <https://doi.org/10.1016/j.tca.2021.178882>
- Bouarab-Chibane L, Forquet V, Lantéri P et al (2019) Antibacterial properties of polyphenols: characterization and QSAR (quantitative structure-activity relationship) models. *Front Microbiol* 10:829. <https://doi.org/10.3389/fmicb.2019.00829>
- Cabezudo I, Meini MR, Di Ponte CC et al (2021) Soybean (*Glycine max*) hull valorization through the extraction of polyphenols by green alternative methods. *Food Chem* 338:128131. <https://doi.org/10.1016/j.foodchem.2020.128131>
- Cagnon B, Py X, Guillot A et al (2009) Contributions of hemi-cellulose, cellulose and lignin to the mass and the porous properties of chars and steam activated carbons from various lignocellulosic precursors. *Bioresour Technol* 100:292–298. <https://doi.org/10.1016/j.biortech.2008.06.009>

- Calza P, Zacchigna D, Laurenti E (2016) Degradation of orange dyes and carbamazepine by soybean peroxidase immobilized on silica monoliths and titanium dioxide. *Environ Sci Pollut Res* 23:23742–23749. <https://doi.org/10.1007/s11356-016-7399-1>
- Camiscia P, Giordano EDV, Brassesco ME et al (2018) Comparison of soybean hull pre-treatments to obtain cellulose and chemical derivatives: physical chemistry characterization. *Carbohydr Polym* 198:601–610. <https://doi.org/10.1016/j.carbpol.2018.06.125>
- Carneiro AM, Moreira EA, Bragagnolo FS et al (2020) Soya agricultural waste as a rich source of isoflavones. *Food Res Int* 130:108949. <https://doi.org/10.1016/j.foodres.2019.108949>
- Carrier M, Loppinet-Serani A, Denux D et al (2011) Thermogravimetric analysis as a new method to determine the lignocellulosic composition of biomass. *Biomass Bioenergy* 35:298–307. <https://doi.org/10.1016/j.biombioe.2010.08.067>
- Chantereau G, Brown N, Dourges MA et al (2019) Silylation of bacterial cellulose to design membranes with intrinsic anti-bacterial properties. *Carbohydr Polym* 220:71–78. <https://doi.org/10.1016/j.carbpol.2019.05.009>
- Chaoui L, Mhand R, Mellouki F, Rhallabi N (2019) Contamination of the surfaces of a health care environment by multidrug-resistant (MDR) bacteria. *Int J Microbiol* 2019:3236526. <https://doi.org/10.1155/2019/3236526>
- Coma V, Freire CSR, Silvestre AJD (2014) Recent advances on the development of antibacterial polysaccharide-based materials. In: Ramawat KG, Mérillon JM (eds) *Polysaccharides*. Springer International Publishing, Cham, pp 1–46
- Credou J, Berthelot T (2014) Cellulose: from biocompatible to bioactive material. *J Mater Chem B* 2:4767–4788. <https://doi.org/10.1039/c4tb00431k>
- Debiagi F, Faria-Tischer PCS, Mali S (2020) Nanofibrillated cellulose obtained from soybean hull using simple and eco-friendly processes based on reactive extrusion. *Cellulose* 27:1975–1988. <https://doi.org/10.1007/s10570-019-02893-0>
- Deghles A, Hamed O, Azai M et al (2019) Cellulose with bidentate chelating functionality: an adsorbent for metal ions from wastewater. *BioResources* 14:6247–6266. <https://doi.org/10.15376/biores.14.3.6247-6266>
- del Carmen Villalobos M, Serradilla MJ, Martín A et al (2016) Antioxidant and antimicrobial activity of natural phenolic extract from defatted soybean flour by-product for stone fruit postharvest application. *J Sci Food Agric* 96:2116–2124. <https://doi.org/10.1002/jsfa.7327>
- Deng C, Seidi F, Yong Q et al (2022) Antiviral/antibacterial biodegradable cellulose nonwovens as environmentally friendly and bioprotective materials with potential to minimize microplastic pollution. *J Hazard Mater* 424:127391. <https://doi.org/10.1016/j.jhazmat.2021.127391>
- Dong Y, Lai Y, Wang X et al (2019) Design and synthesis of amine-functionalized cellulose with multiple binding sites and their application in C–C bond forming reactions. *Int J Biol Macromol* 130:778–785. <https://doi.org/10.1016/j.ijbiomac.2019.02.158>
- Dufresne A (2017) *Handbook of nanocellulose and cellulose nanocomposites*. Wiley-VCH Verlag, Weinheim
- Durkin DP, Frank BP, Haverhals LM et al (2019) Engineering lignocellulose fibers with higher thermal stability through natural fiber welding. *Macromol Mater Eng* 304:1900042. <https://doi.org/10.1002/mame.201900042>
- Esparza-González SC, Sánchez-Valdés S, Ramírez-Barrón SN et al (2016) Effects of different surface modifying agents on the cytotoxic and antimicrobial properties of ZnO nanoparticles. *Toxicol In Vitro* 37:134–141. <https://doi.org/10.1016/j.tiv.2016.09.020>
- Espino-Pérez E, Domenek S, Belgacem N et al (2014) Green process for chemical functionalization of nanocellulose with carboxylic acids. *Biomacromolecules* 15:4551–4560. <https://doi.org/10.1021/bm5013458>
- Ferrer A, Salas C, Rojas OJ (2016) Physical, thermal, chemical and rheological characterization of cellulosic microfibrils and microparticles produced from soybean hulls. *Ind Crops Prod* 84:337–343. <https://doi.org/10.1016/j.indcrop.2016.02.014>
- Flauzino Neto WP, Silvério HA, Dantas NO, Pasquini D (2013) Extraction and characterization of cellulose nanocrystals from agro-industrial residue-soy hulls. *Ind Crops Prod* 42:480–488. <https://doi.org/10.1016/j.indcrop.2012.06.041>
- French AD (2014) Idealized powder diffraction patterns for cellulose polymorphs. *Cellulose* 21:885–896. <https://doi.org/10.1007/s10570-013-0030-4>
- French AD (2017) Glucose, not cellobiose, is the repeating unit of cellulose and why that is important. *Cellulose* 24:4605–4609. <https://doi.org/10.1007/s10570-017-1450-3>
- Gao L, Wang H, Zheng B, Huang F (2021) Combating antibiotic resistance: current strategies for the discovery of novel antibacterial materials based on macrocycle supramolecular chemistry. *Giant* 7:100066. <https://doi.org/10.1016/j.giant.2021.100066>
- Gao M, Shang Y, Li B, Du H (2022) Sustainable preparation of cellulose nanocrystals: state of the art and perspectives. *Green Chem* 24:9346–9372. <https://doi.org/10.1039/D2GC03003A>
- García-Maraver A, Salvachúa D, Martínez MJ et al (2013) Analysis of the relation between the cellulose, hemicellulose and lignin content and the thermal behavior of residual biomass from olive trees. *Waste Manag* 33:2245–2249. <https://doi.org/10.1016/j.wasman.2013.07.010>
- Ghasemi M, Tsianou M, Alexandridis P (2017) Assessment of solvents for cellulose dissolution. *Bioresour Technol* 228:330–338. <https://doi.org/10.1016/j.biortech.2016.12.049>
- Gong J, Li J, Xu J et al (2017) Research on cellulose nanocrystals produced from cellulose sources with various polymorphs. *RSC Adv* 7:33486–33493. <https://doi.org/10.1039/c7ra06222b>
- Guimarães AC, Meireles LM, Lemos MF et al (2019) Antibacterial activity of terpenes and terpenoids present in essential oils. *Molecules* 24:1–12. <https://doi.org/10.3390/molecules24132471>

- Habibi Y (2014) Key advances in the chemical modification of nanocelluloses. *Chem Soc Rev* 43:1519–1542. <https://doi.org/10.1039/c3cs60204d>
- Hassanpour A, Asghari S, Lakouraj MM (2017) Synthesis, characterization and antibacterial evaluation of nanofibrillated cellulose grafted by a novel quinolinium silane salt. *RSC Adv* 7:23907–23916. <https://doi.org/10.1039/c7ra02765f>
- Hassanpour A, Asghari S, Mansour Lakouraj M, Mohseni M (2018) Preparation and characterization of contact active antibacterial surface based on chemically modified nanofibrillated cellulose by phenanthridinium silane salt. *Int J Biol Macromol* 115:528–539. <https://doi.org/10.1016/j.ijbiomac.2018.03.141>
- Heinze T, Liebert T (2001) Unconventional methods in cellulose functionalization. *Prog Polym Sci* 26:1689–1762
- Helmiyati SA, Yulianti W (2014) Synthesis and swelling kinetics of superabsorbent rice straw cellulose graft copolymers. *Asian J Chem* 26:7337–7342. <https://doi.org/10.14233/ajchem.2014.16754>
- Hosseini Chaleshtori SA, Ataie Kachoe M, Hashemi Jazi SM (2017) Antibacterial effects of the methanolic extract of *Glycine Max* (soybean). *Microbiol Res (Pavia)* 8:51–54. <https://doi.org/10.4081/mr.2017.7319>
- Huang W, Tao F, Li F et al (2020) Antibacterial nanomaterials for environmental and consumer product applications. *NanoImpact* 20:100268. <https://doi.org/10.1016/j.impact.2020.100268>
- Hudson-Mcaulay K, Kennedy CJ, Jarvis MC (2020) Chemical and mechanical differences between historic and modern scots pine wood. *Heritage* 3:116–127. <https://doi.org/10.3390/heritage3010007>
- Ielo I, Giacobello F, Castellano A et al (2021) Development of antibacterial and antifouling innovative and eco-sustainable sol–gel based materials: from marine areas protection to healthcare applications. *Gels* 8:26. <https://doi.org/10.3390/gels8010026>
- Iglesias MC, Hamade F, Aksoy B et al (2021) Correlations between rheological behavior and intrinsic properties of nanofibrillated cellulose from wood and soybean hulls with varying lignin content. *BioResources* 16:4831–4845. <https://doi.org/10.15376/biores.16.3.4831-4845>
- Jaekel EE, Sirviö JA, Antonietti M, Filonenko S (2021) One-step method for the preparation of cationic nanocellulose in reactive eutectic media. *Green Chem* 23:2317–2323. <https://doi.org/10.1039/d0gc04282j>
- Jiang Y, Liu X, Yang Q et al (2019) Effects of residual lignin on composition, structure and properties of mechanically defibrillated cellulose fibrils and films. *Cellulose* 26:1577–1593. <https://doi.org/10.1007/s10570-018-02229-4>
- Jungnickl K, Paris O, Fratzl P, Burgert I (2008) The implication of chemical extraction treatments on the cell wall nanostructure of softwood. *Cellulose* 15:407–418. <https://doi.org/10.1007/s10570-007-9181-5>
- Juntaro J, Ummartyotin S, Sain M, Manuspiya H (2012) Bacterial cellulose reinforced polyurethane-based resin nanocomposite: a study of how ethanol and processing pressure affect physical, mechanical and dielectric properties. *Carbohydr Polym* 87:2464–2469. <https://doi.org/10.1016/j.carbpol.2011.11.020>
- Kedzior SA, Zoppe JO, Berry RM, Cranston ED (2019) Recent advances and an industrial perspective of cellulose nanocrystal functionalization through polymer grafting. *Curr Opin Solid State Mater Sci* 23:74–91. <https://doi.org/10.1016/j.cossms.2018.11.005>
- Khanjanzadeh H, Behrooz R, Bahramifar N et al (2018) Surface chemical functionalization of cellulose nanocrystals by 3-aminopropyltriethoxysilane. *Int J Biol Macromol* 106:1288–1296. <https://doi.org/10.1016/j.ijbiomac.2017.08.136>
- Khattak S, Wahid F, Liu LP et al (2019) Applications of cellulose and chitin/chitosan derivatives and composites as antibacterial materials: current state and perspectives. *Appl Microbiol Biotechnol* 103:1989–2006. <https://doi.org/10.1007/s00253-018-09602-0>
- Korntner P, Hosoya T, Dietz T et al (2015) Chromophores in lignin-free cellulosic materials belong to three compound classes. *Chromophores in cellulose, XII. Cellulose* 22:1053–1062. <https://doi.org/10.1007/s10570-015-0566-6>
- Koshani R, Eiyegbenin JE, Wang Y, van de Ven TGM (2022) Synthesis and characterization of hairy aminated nanocrystalline cellulose. *J Colloid Interface Sci* 607:134–144. <https://doi.org/10.1016/j.jcis.2021.08.172>
- Kumar Gupta K, Sai Raghunath S, Venkatesh Prasanna D et al (2019) An update on overview of cellulose, its structure and applications. In: *Cellulose*. IntechOpen. <https://doi.org/10.5772/intechopen.84727>
- Kusi J, Ojewole CO, Ojewole AE, Nwi-Mozu I (2022) Antimicrobial resistance development pathways in surface waters and public health implications. *Antibiotics* 11:1–22. <https://doi.org/10.3390/antibiotics11060821>
- Kwiczak-Yigitbaşı J, Laçın Ö, Demir M et al (2020) A sustainable preparation of catalytically active and antibacterial cellulose metal nanocomposites: via ball milling of cellulose. *Green Chem* 22:455–464. <https://doi.org/10.1039/c9gc02781e>
- Lavagna L, Tummino ML, Magnacca G et al (2021) Immobilized bi-enzymatic system for the determination of biogenic amines in solution. *Biochem Eng J* 169:107960. <https://doi.org/10.1016/j.bej.2021.107960>
- Leong AJ, Nyuk-Ting N, Nor NSM et al (2019) Removal of rhodamine 6G and crystal violet dyes from water sample using cellulose acetate-(3-aminopropyl)-triethoxysilane sorbent. *AIP Conf Proc* 2155:020013. <https://doi.org/10.1063/1.5125517>
- Li J, Zhuang S (2020) Antibacterial activity of chitosan and its derivatives and their interaction mechanism with bacteria: current state and perspectives. *Eur Polym J* 138:109984. <https://doi.org/10.1016/j.eurpolymj.2020.109984>
- Liang J, Chen J, Wu S et al (2018) Comprehensive insights into cellulose structure evolution: via multi-perspective analysis during a slow pyrolysis process. *Sustain Energy Fuels* 2:1855–1862. <https://doi.org/10.1039/c8se00166a>
- Liguori K, Keenum I, Davis BC et al (2022) Antimicrobial resistance monitoring of water environments: a framework for standardized methods and quality control. *Environ Sci Technol* 56:9149–9160. <https://doi.org/10.1021/acs.est.1c08918>

- Liyanage S, Acharya S, Parajuli P et al (2021) Production and surface modification of cellulose bioproducts. *Polymers (Basel)* 13:3433. <https://doi.org/10.3390/polym13193433>
- Lopez-Romero JC, González-Ríos H, Borges A, Simões M (2015) Antibacterial effects and mode of action of selected essential oils components against *Escherichia coli* and *Staphylococcus aureus*. *Evid Based Complement Altern Med* 2015:795435. <https://doi.org/10.1155/2015/795435>
- Lu Z, Dockery CR, Crosby M et al (2016) Antibacterial activities of wasabi against *Escherichia coli* O157: H7 and *Staphylococcus aureus*. *Front Microbiol* 7:1–9. <https://doi.org/10.3389/fmicb.2016.01403>
- Luo H, Jiang YZ, Tan L (2022) Positively-charged microcrystalline cellulose microparticles: rapid killing effect on bacteria, trapping behavior and excellent elimination efficiency of biofilm matrix from water environment. *J Hazard Mater* 424:127299. <https://doi.org/10.1016/j.jhazmat.2021.127299>
- Mahira S, Jain A, Khan W, Domb AJ (2019) Chapter 1. Antimicrobial materials—an overview. In: *Antimicrobial materials for biomedical applications*, ed. A. J. Domb, K. R. Kunduru, and S. Farah, The Royal Society of Chemistry, pp 1–37. <https://doi.org/10.1039/9781788012638-00001>
- Maruthapandi M, Saravanan A, Gupta A et al (2022) Antimicrobial activities of conducting polymers and their composites. *Macromol* 2:78–99. <https://doi.org/10.3390/macromol2010005>
- Merci A, Urbano A, Grossmann MVE et al (2015) Properties of microcrystalline cellulose extracted from soybean hulls by reactive extrusion. *Food Res Int* 73:38–43. <https://doi.org/10.1016/j.foodres.2015.03.020>
- Morán JI, Alvarez VA, Cyras VP, Vázquez A (2008) Extraction of cellulose and preparation of nanocellulose from sisal fibers. *Cellulose* 15:149–159. <https://doi.org/10.1007/s10570-007-9145-9>
- Muley PD, Henkel C, Abdollahi KK et al (2016) A critical comparison of pyrolysis of cellulose, lignin, and pine sawdust using an induction heating reactor. *Energy Convers Manag* 117:273–280. <https://doi.org/10.1016/j.enconman.2016.03.041>
- Muñoz-Bonilla A, Echeverría C, Sonseca Á et al (2019) Bio-based polymers with antimicrobial properties towards sustainable development. *Materials (Basel)* 12:641. <https://doi.org/10.3390/ma12040641>
- Muqet M, Mahar RB, Gadhi TA, Ben Halima N (2020) Insight into cellulose-based-nanomaterials: a pursuit of environmental remedies. *Int J Biol Macromol* 163:1480–1486. <https://doi.org/10.1016/j.ijbiomac.2020.08.050>
- Musee N, Thwala M, Nota N (2011) The antibacterial effects of engineered nanomaterials: implications for wastewater treatment plants. *J Environ Monit* 13:1164–1183. <https://doi.org/10.1039/c1em10023h>
- Naz S, Ahmad N, Akhtar J et al (2016) Management of citrus waste by switching in the production of nanocellulose. *IET Nanobiotechnol* 10:395–399. <https://doi.org/10.1049/iet-nbt.2015.0116>
- Nemeş NS, Ardean C, Davidescu CM et al (2022) Antimicrobial activity of cellulose based materials. *Polymers (Basel)* 14:8–12. <https://doi.org/10.3390/polym14040735>
- Neves RM, Ornaghi HL, Zattera AJ, Amico SC (2020) The influence of silane surface modification on microcrystalline cellulose characteristics. *Carbohydr Polym* 230:115595. <https://doi.org/10.1016/j.carbpol.2019.115595>
- Nile SH, Nile A, Oh JW, Kai G (2020) Soybean processing waste: potential antioxidant, cytotoxic and enzyme inhibitory activities. *Food Biosci* 38:100778. <https://doi.org/10.1016/j.fbio.2020.100778>
- Nile SH, Venkidasamy B, Samynathan R et al (2022) Soybean processing wastes: novel insights on their production, extraction of Isoflavones, and their therapeutic Properties. *J Agric Food Chem* 70:6849–6863. <https://doi.org/10.1021/acs.jafc.1c04927>
- Niño-Medina G, Muy-Rangel D, Urías-Orona V (2017) Chickpea (*Cicer arietinum*) and soybean (*Glycine max*) Hulls: byproducts with potential use as a source of high value-added food products. *Waste Biomass Valoriz* 8:1199–1203. <https://doi.org/10.1007/s12649-016-9700-4>
- Noremlyia MB, Hassan MZ, Ismail Z (2022) Recent advancement in isolation, processing, characterization and applications of emerging nanocellulose: a review. *Int J Biol Macromol* 206:954–976. <https://doi.org/10.1016/j.ijbiomac.2022.03.064>
- Park S, Baker JO, Himmel ME et al (2010) Cellulose crystallinity index: measurement techniques and their impact on interpreting cellulase performance. *Biotechnol Biofuels* 3:10. <https://doi.org/10.1186/1754-6834-3-10>
- Phanthong P, Reubroycharoen P, Hao X et al (2018) Nanocellulose: extraction and application. *Carbon Resour Convers* 1:32–43. <https://doi.org/10.1016/j.crcon.2018.05.004>
- Poletto M, Pistor V, Zattera AJ (2013) Structural characteristics and thermal properties of native cellulose. In: *Cellulose—fundamental aspects*. InTech. <https://doi.org/10.5772/50452>
- Pradhan D, Jaiswal AK, Jaiswal S (2022) Emerging technologies for the production of nanocellulose from lignocellulosic biomass. *Carbohydr Polym* 285:119258. <https://doi.org/10.1016/j.carbpol.2022.119258>
- Radotić K, Mičić M (2016) Methods for extraction and purification of lignin and cellulose from plant tissues. In: *Sample preparation techniques for soil, plant, and animal samples*, ed. Mičić M, Springer Protocols Handbooks, pp 365–376. https://doi.org/10.1007/978-1-4939-3185-9_26
- Rana AK, Frollini E, Thakur VK (2021) Cellulose nanocrystals: pretreatments, preparation strategies, and surface functionalization. *Int J Biol Macromol* 182:1554–1581. <https://doi.org/10.1016/j.ijbiomac.2021.05.119>
- Rashid S, Dutta H (2022) Industrial applications of cellulose extracted from agricultural and food industry wastes. In: *Handbook of biomass valorization for industrial applications*, ed. Shahid-ul-Islam, A.H. Shalla and S.A. Khan, Wiley, p 417–443. <https://doi.org/10.1002/9781119818816.ch18>
- Rashki S, Shakour N, Yousefi Z et al (2021) Cellulose-based nanofibril composite materials as a new approach to fight bacterial infections. *Front Bioeng Biotechnol* 9:1–16. <https://doi.org/10.3389/fbioe.2021.732461>

- Reshmy R, Philip E, Paul SA et al (2020) Nanocellulose-based products for sustainable applications-recent trends and possibilities. *Rev Environ Sci Biotechnol* 19:779–806. <https://doi.org/10.1007/s11157-020-09551-z>
- Robles E, Csóka L, Labidi J (2018) Effect of reaction conditions on the surface modification of cellulose nanofibrils with aminopropyl triethoxysilane. *Coatings* 8:139. <https://doi.org/10.3390/coatings8040139>
- Rosa SML, Rehman N, De Miranda MIG et al (2012) Chlorine-free extraction of cellulose from rice husk and whisker isolation. *Carbohydr Polym* 87:1131–1138. <https://doi.org/10.1016/j.carbpol.2011.08.084>
- Rosenau T, Potthast A, Hofinger A, Kosma P (2005) Isolation and identification of residual chromophores in cellulosic materials. *Macromol Symp* 223:239–252. <https://doi.org/10.1002/masy.200550517>
- Samrot AV, Ngaakudzwe KT, Rajalakshmi D et al (2022) Waste-derived cellulosic fibers and their applications. *Adv Mater Sci Eng* 2022:7314694. <https://doi.org/10.1155/2022/7314694>
- Seddiqi H, Oliaei E, Honarkar H et al (2021) Cellulose and its derivatives: towards biomedical applications. *Cellulose* 28:1893–1931. <https://doi.org/10.1007/s10570-020-03674-w>
- Shao W, Wu J, Liu H et al (2017) Novel bioactive surface functionalization of bacterial cellulose membrane. *Carbohydr Polym* 178:270–276. <https://doi.org/10.1016/j.carbpol.2017.09.045>
- Sheltami RM, Kargarzadeh H, Abdullah I (2015) Effects of silane surface treatment of cellulose nanocrystals on the tensile properties of cellulose-polyvinyl chloride nanocomposite. *Sains Malays* 44:801–810. <https://doi.org/10.17576/jsm-2015-4406-05>
- Shi X, Wang S, Wen S et al (2011) Aminopropyltriethoxysilane-mediated surface functionalization of hydroxyapatite nanoparticles: synthesis, characterization, and in vitro toxicity assay. *Int J Nanomed* 6:3449–3459. <https://doi.org/10.2147/IJN.S27166>
- Shokri J, Adibki K (2013) Application of cellulose and cellulose derivatives in pharmaceutical industries. In: *Cellulose—medical, pharmaceutical and electronic applications*. IntechOpen. <https://doi.org/10.5772/55178>
- Siedenbiedel F, Tiller JC (2012) Antimicrobial polymers in solution and on surfaces: overview and functional principles. *Polymers (Basel)* 4:46–71. <https://doi.org/10.3390/polym4010046>
- Sinclair A, Jiang L, Bajwa D et al (2018) Cellulose nanofibers produced from various agricultural residues and their reinforcement effects in polymer nanocomposites. *J Appl Polym Sci* 135:9–11. <https://doi.org/10.1002/app.46304>
- Sperandeo P, Bosco F, Clerici F et al (2020) Covalent grafting of antimicrobial peptides onto microcrystalline cellulose. *ACS Appl Bio Mater* 3:4895–4901. <https://doi.org/10.1021/acsabm.0c00412>
- Srivastav AL, Patel N, Chaudhary VK (2020) Disinfection by-products in drinking water: occurrence, toxicity and abatement. *Environ Pollut* 267:115474. <https://doi.org/10.1016/j.envpol.2020.115474>
- Stepanova M, Korzhikova-Vlakh E (2022) Modification of cellulose micro- and nanomaterials to improve properties of aliphatic polyesters/cellulose composites: a review. *Polymers (Basel)* 14:1477. <https://doi.org/10.3390/polym14071477>
- Tang Z, Bian S, Lin Z et al (2021) Biocompatible catechol-functionalized cellulose-based adhesives with strong water resistance. *Macromol Mater Eng* 306:1–10. <https://doi.org/10.1002/mame.202100232>
- Testa ML (2021) Functionalized nanomaterials for biomass conversion. *Mater Today Proc* 35:156–163. <https://doi.org/10.1016/j.matpr.2020.04.064>
- Testa ML, La Parola V (2021) Sulfonic acid-functionalized inorganic materials as efficient catalysts in various applications: a minireview. *Catalysts* 11:1143. <https://doi.org/10.3390/catal11101143>
- Testa ML, Tummino ML (2021) Lignocellulose biomass as a multifunctional tool for sustainable catalysis and chemicals: an overview. *Catalysts* 11:125. <https://doi.org/10.3390/catal11010125>
- Testa ML, Tummino ML, Agostini S et al (2015) Synthesis, characterization and environmental application of silica grafted photoactive substances isolated from urban bio-waste. *RSC Adv* 5:47920–47927. <https://doi.org/10.1039/C5RA03164H>
- Trache D, Hussin MH, Hui Chuin CT et al (2016) Microcrystalline cellulose: isolation, characterization and bio-composites application—a review. *Int J Biol Macromol* 93:789–804. <https://doi.org/10.1016/j.ijbiomac.2016.09.056>
- Trache D, Tarchoun AF, Derradji M et al (2020) Nanocellulose: from fundamentals to advanced applications. *Front Chem* 8:392. <https://doi.org/10.3389/fchem.2020.00392>
- Tummino ML, Testa ML, Malandrino M et al (2019) Green waste-derived substances immobilized on SBA-15 silica: surface properties, adsorbing and photosensitizing activities towards organic and inorganic substrates. *Nanomaterials* 9:162. <https://doi.org/10.3390/nano9020162>
- Tummino ML, Tolardo V, Malandrino M et al (2020) A way to close the loop: physicochemical and adsorbing properties of soybean hulls recovered after soybean peroxidase extraction. *Front Chem* 8:763. <https://doi.org/10.3389/fchem.2020.00763>
- Tyagi P, Mathew R, Opperman C et al (2019) High-strength antibacterial chitosan-cellulose nanocrystal composite tissue paper. *Langmuir* 35:104–112. <https://doi.org/10.1021/acs.langmuir.8b02655>
- Varghese AG, Paul SA, Latha MS (2019) Remediation of heavy metals and dyes from wastewater using cellulose-based adsorbents. *Environ Chem Lett* 17:867–877. <https://doi.org/10.1007/s10311-018-00843-z>
- Voicu SI, Thakur VK (2021) Aminopropyltriethoxysilane as a linker for cellulose-based functional materials: new horizons and future challenges. *Curr Opin Green Sustain Chem* 30:100480. <https://doi.org/10.1016/j.cogsc.2021.100480>
- Wang J, Minami E, Kawamoto H (2020) Thermal reactivity of hemicellulose and cellulose in cedar and beech wood cell walls. *J Wood Sci* 66:41. <https://doi.org/10.1186/s10086-020-01888-x>
- Wu S, Shi W, Li K et al (2022) Recent advances on sustainable bio-based materials for water treatment: fabrication, modification and application. *J Environ Chem Eng* 10:108921. <https://doi.org/10.1016/j.jece.2022.108921>

- Yang Q, Pan X (2010) A facile approach for fabricating fluorescent cellulose. *J Appl Polym Sci* 117:3639–3644. <https://doi.org/10.1002/app.32287>
- Yang H, Yan R, Chen H et al (2007) Characteristics of hemicellulose, cellulose and lignin pyrolysis. *Fuel* 86:1781–1788. <https://doi.org/10.1016/j.fuel.2006.12.013>
- Yang YP, Zhang Y, Lang YX, Yu MH (2017) Structural ATR-IR analysis of cellulose fibers prepared from a NaOH complex aqueous solution. *IOP Conf Ser Mater Sci Eng* 213:012039. <https://doi.org/10.1088/1757-899X/213/1/012039>
- Zardini HZ, Amiri A, Shanbedi M et al (2012) Enhanced antibacterial activity of amino acids-functionalized multi walled carbon nanotubes by a simple method. *Colloids Surf B Biointerfaces* 92:196–202. <https://doi.org/10.1016/j.colsurfb.2011.11.045>
- Zhang S, Xia C, Dong Y et al (2016) Soy protein isolate-based films reinforced by surface modified cellulose nanocrystal. *Ind Crops Prod* 80:207–213. <https://doi.org/10.1016/j.indcrop.2015.11.070>
- Zhang N, Tao P, Lu Y, Nie S (2019) Effect of lignin on the thermal stability of cellulose nanofibrils produced from bagasse pulp. *Cellulose* 26:7823–7835. <https://doi.org/10.1007/s10570-019-02657-w>
- Zhang B, Zhang Y, Li H et al (2020) A review on insoluble-bound phenolics in plant-based food matrix and their contribution to human health with future perspectives. *Trends Food Sci Technol* 105:347–362. <https://doi.org/10.1016/j.tifs.2020.09.029>
- Zhang Y, Wang H, Sun X et al (2021) Separation and characterization of biomass components (cellulose, hemicellulose, and lignin) from corn stalk. *BioResources* 16:7205–7219. <https://doi.org/10.15376/biores.16.4.7205-7219>
- Zheng A, Li L, Zhao Z et al (2021) Effect of torrefaction pretreatment on chemical structure and pyrolysis behaviors of cellulose. *IOP Conf Ser Earth Environ Sci* 621:012014. <https://doi.org/10.1088/1755-1315/621/1/012014>

Publisher's Note Springer Nature remains neutral with regard to jurisdictional claims in published maps and institutional affiliations.